

Electronic Supplementary Information for:

**Encryption application of fast stimulus-responsive hydrogen-bonded
organic framework based on FRET**

Bing-Sha Li,^a Li-Hui Cao, ^{*a} Xu-Yong Chen,^a Yu Tian^{*a}

^aShaanxi Key Laboratory of Chemical Additives for Industry, College of Chemistry and Chemical Engineering, Shaanxi University of Science and Technology, Xi'an, 710021, P. R. China

E-mail: caolihui@sust.edu.cn, tianyu@sust.edu.cn

Experimental section

Materials and reagents.

All reagents and solvents, including Naphthalene-1,4,5,8-tetracarboxylic dianhydride (NDI), terephthalimidine dihydrochloride (PAM·2HCl), L-Phenyl Alanine, polyvinyl alcohol (PVA), acetic acid and *N,N'*-dimethylformamide (DMF) were obtained from the commercial companies and used without further purification. Deionized water was used throughout all experiments wherever is needed.

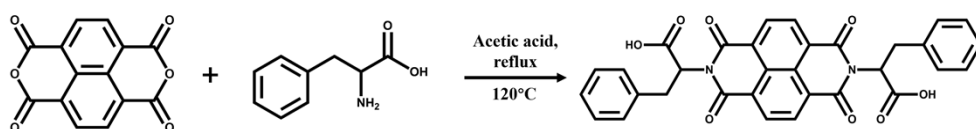
Characterization.

Powder X-ray diffraction (PXRD) measurements were carried out in Bruker D8 Advance with a Cu X-ray source over a range of $2\theta = 5.0\sim 50.0^\circ$. The Fourier transform infrared (FT-IR) spectra (KBr pellets) were recorded in the range of $500\text{--}4000\text{ cm}^{-1}$ on a VECTOR-22 spectrograph. The solid-state UV-vis spectra were obtained from a Cary 5000 spectrophotometer. Fluorescence spectra were recorded on an Edinburgh FLS-1000 fluorescence spectrometer. ^1H NMR spectra was recorded on a Bruker-600 MHz spectrometer with chemical shifts reported as ppm. Thermogravimetric analysis (TGA) measurements were performed on a TGA-55 instrument from $25\text{ }^\circ\text{C}$ to $800\text{ }^\circ\text{C}$ at a heating rate of $10\text{ }^\circ\text{C}/\text{min}$ under N_2 atmosphere. Scanning electron microscope tests were performed

on a SU8100. X-ray photoelectron spectroscopy (XPS) was obtained by AXIS SUPRA X-ray photoelectron spectrometer and the C 1s peak at 284.8 eV as internal standard. The solid-state EPR spectra were recorded at ambient temperature with a Bruker A300 Electron Spin Resonance Spectrometer.

Preparation of ligand (H₂PheNDI).

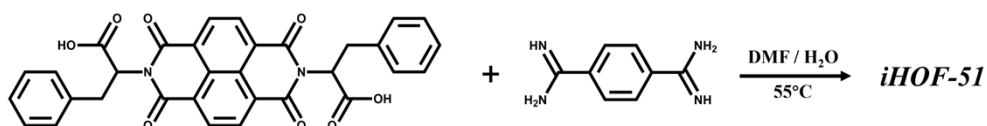
Phenylalanine substituted naphthalene diimide ligand (H₂PheNDI) was synthesized by the method reported in the literature. A mixture of naphthalene-1,4,5,8-tetracarboxylic dianhydride (5 g, 18.6 mmol) and L-Phenyl Alanine (6.47g, 39.2mmol) was refluxed in 127 mL acetic acid for 36 h at a reaction temperature of 120°C. The resulting brown coloured reaction mixture was concentrated under reduced pressure and diluted with excess amount of deionised water to give final product as a brown precipitate. The resulting solution was filtered off and dried under vacuum to obtain desired product. Yield 9.5g, ~91% . It is hypothesized that perhaps during the synthesis process, the acid was added in excess making it possible for the chiral ligand to undergo racemization, resulting in the loss of chirality. Therefore, the synthesized H₂PheNDI ligand done in this paper is without chirality.¹



Scheme S1. Schematic representation for preparation of compound H₂PheNDI.

Preparation of iHOF-51.

H₂PheNDI (6.5 mg, 11.6 mmol) was dissolved in 2 mL of DMF to ensure complete dissolution. Subsequently, PAM·2HCl (8 mg, 14.2 mmol) was dissolved in 2.5 mL of water to form a clarified solution. Next, the above two clarified solutions were mixed thoroughly and placed in an oven at 55°C for 7 days. During this process, the mixed solution was sealed with plastic wrap and several small holes were tied to slowly evaporate the solvent. Eventually, light yellow transparent square crystals will be obtained.



Scheme S2. Schematic representation for preparation of compound iHOF-51.

Preparation of 1%- iHOF-51-PVA composite membrane.

10 wt % PVA (0.2 g) was added to 2 mL water and stirred for 3 hour to form a good dispersion, and then iHOF-51 (2 mg) was fully ground and

added to 2 mL water and stirred for 3 hours to obtain a well-dispersed suspension. Mix the two together and stir continuously at room temperature for 12 hours to obtain a homogeneous solution. The resulting mixed solution was poured onto a glass mold and dried at room temperature for 48 hours to remove the solvent, resulting in a **1%-iHOF-51-PVA** composite membrane.²

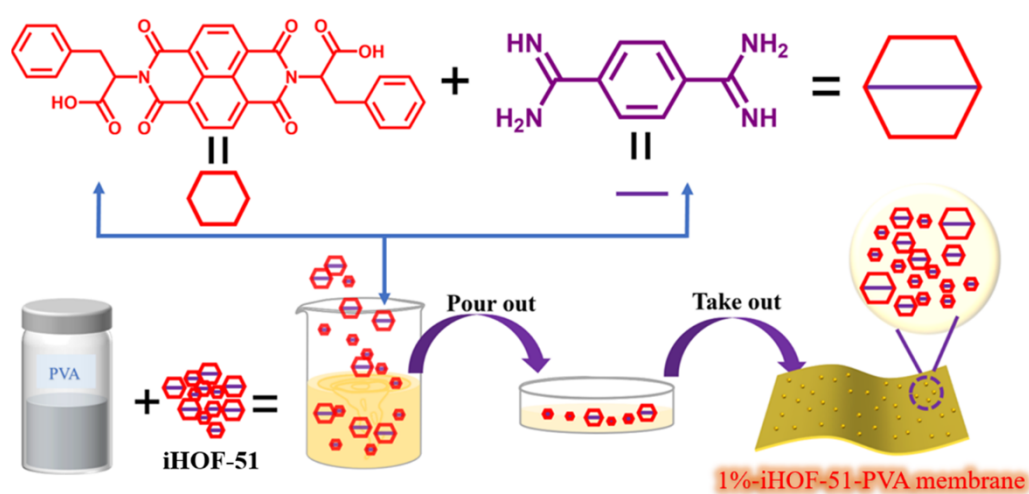


Figure S1. The 1%- iHOF-51-PVA composite membrane production process.

Single-Crystal X-ray Diffraction.

Single-crystal X-ray diffraction data for compound **iHOF-51** was collected on a Bruker SMART APEX CCD diffractometer equipped with graphite-monochromated Mo-K α radiation ($\lambda = 0.71073 \text{ \AA}$) using the ω -scan technique. Data reduction was performed using SAINT and corrected for Lorentz and polarization effects. Adsorption corrections were applied using the SADABS routine.³ All the structures were solved with direct methods (SHELXS) and refined by full-matrix least squares on F² using OLEX2, which utilizes the SHELXL-2015 module.⁴ All non-hydrogen atoms were refined anisotropically. Displacement parameter restraints were used in modeling the ligands. Hydrogen atoms were placed geometrically on their riding atom where possible. The contents of the solvent region are not represented in the unit cell contents in the crystal data. Crystal data containing space group, lattice parameters and other relevant information for the title complex are summarized in Table S1. More details on the crystallographic data are given in the X-ray crystallographic files in CIF format. Full details of the structure determinations have been deposited with Cambridge Crystallographic Data Center under reference number CCDC 2424540 for **iHOF-51**.

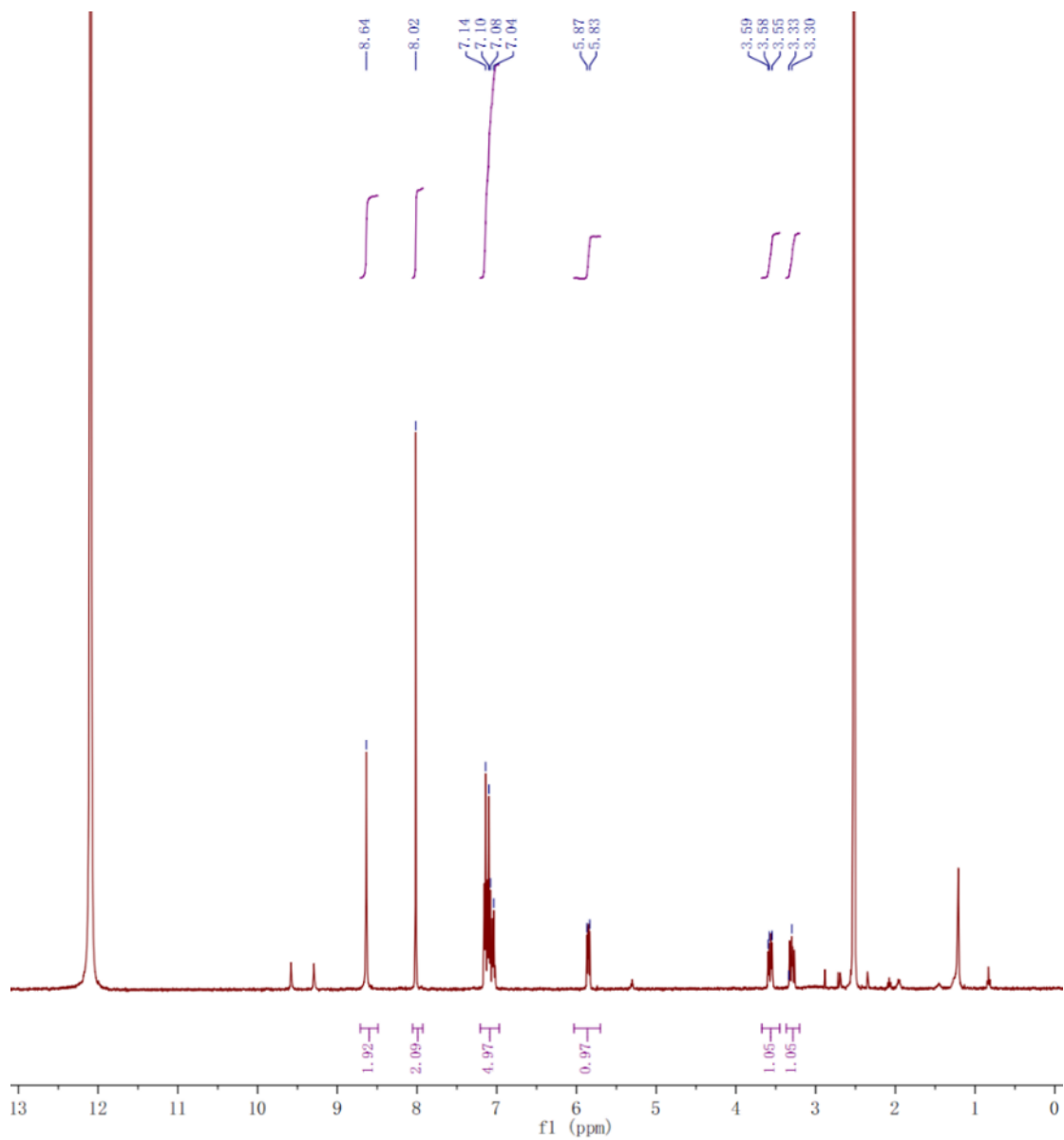


Figure S2. ¹H NMR spectrum of iHOF-51.

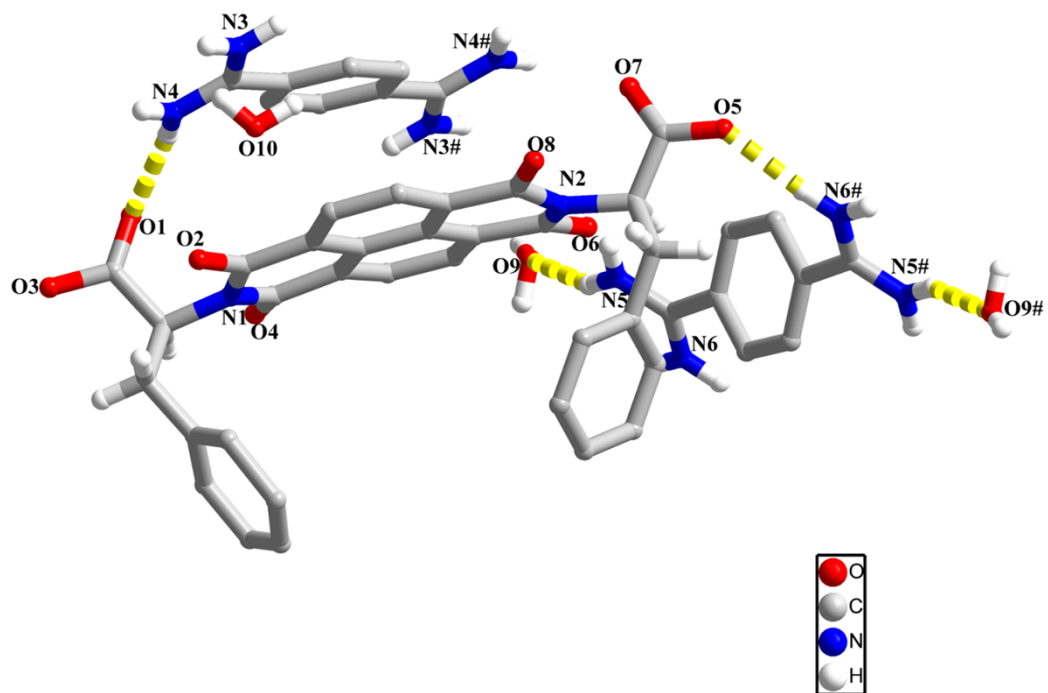


Figure S3. The asymmetric unit of **iHOF-51**. The H atoms are omitted for clarity.

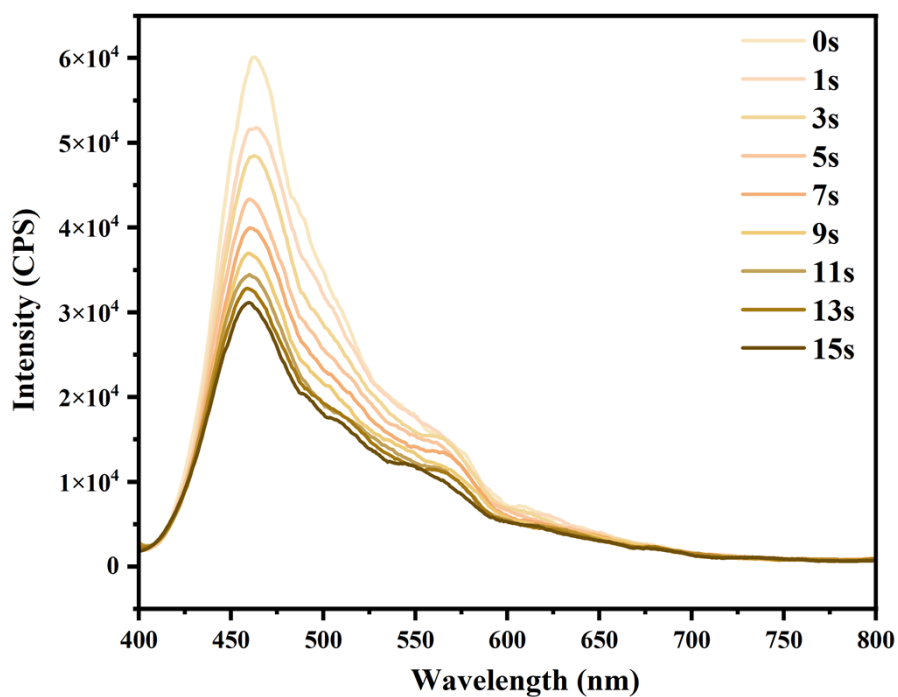


Figure S4. Time-dependent photoluminescence spectra of **iHOF-51** before and after illumination ($\lambda_{\text{ex}}=365$ nm).

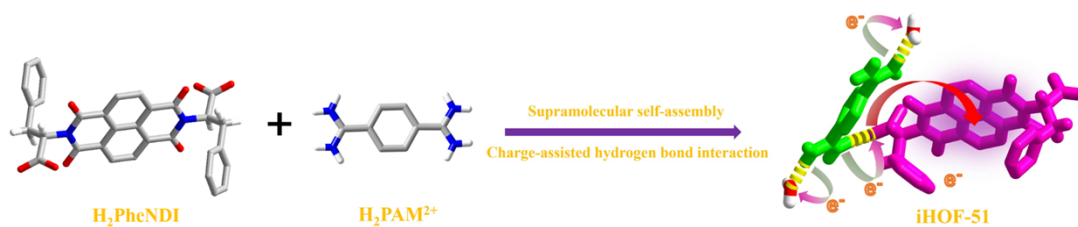


Figure S5. The putative pathway for electron transfer via hydrogen bonding in **iHOF-51**.

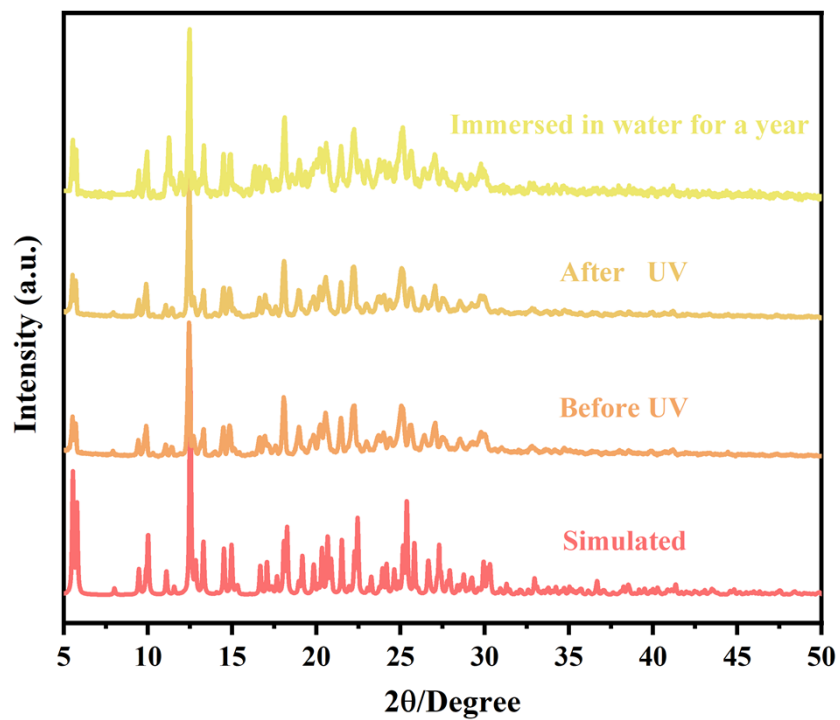


Figure S6. PXRD patterns of iHOF-51.

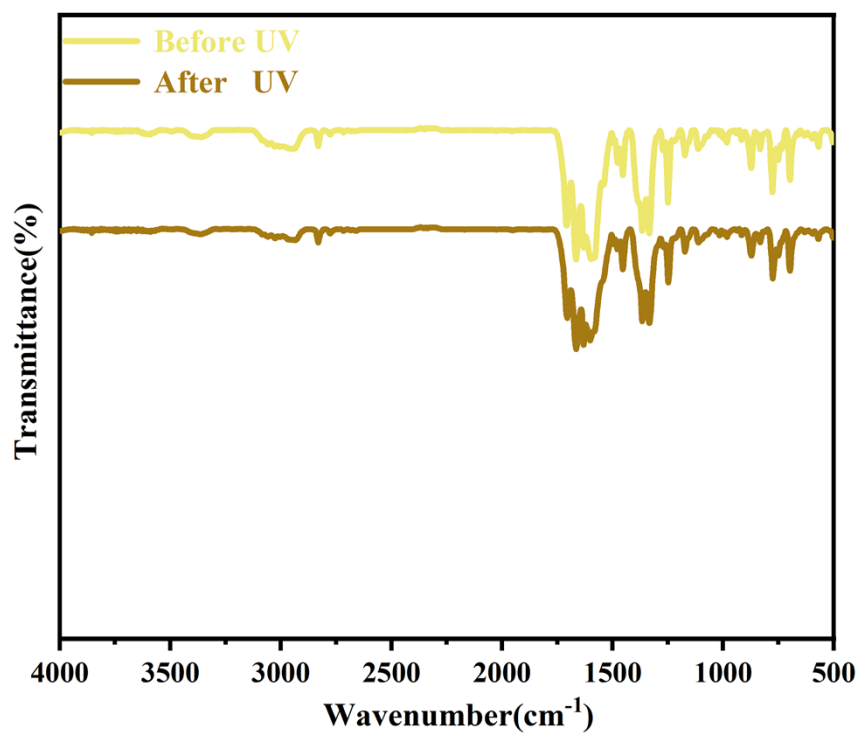


Figure S7. IR spectra of iHOF-51.

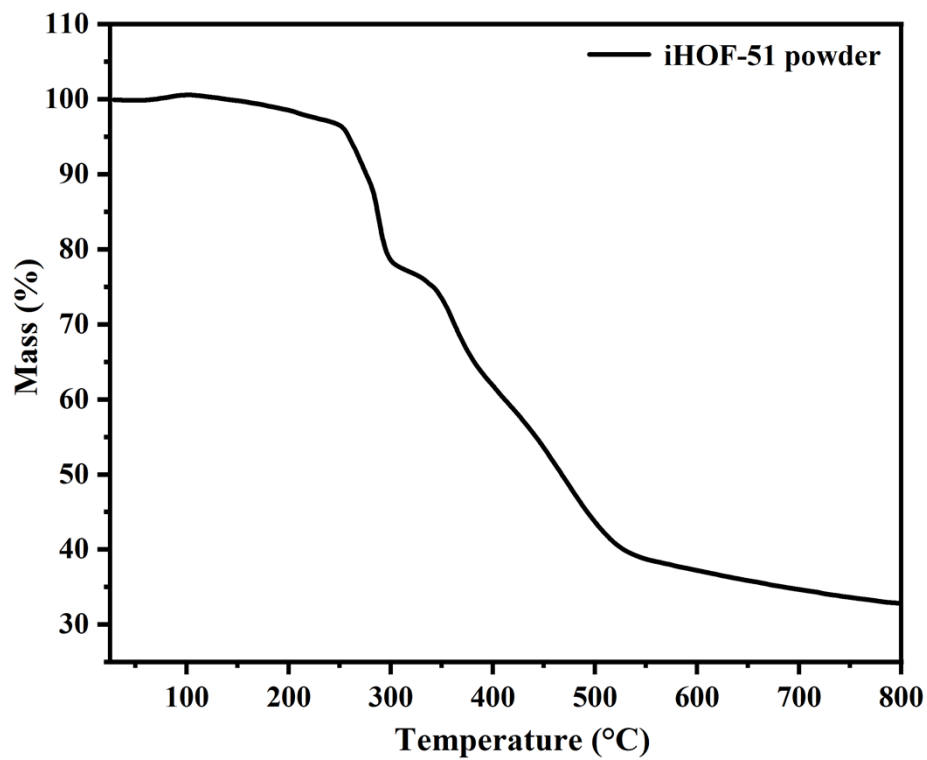


Figure S8. TGA plot of iHOF-51 powder.

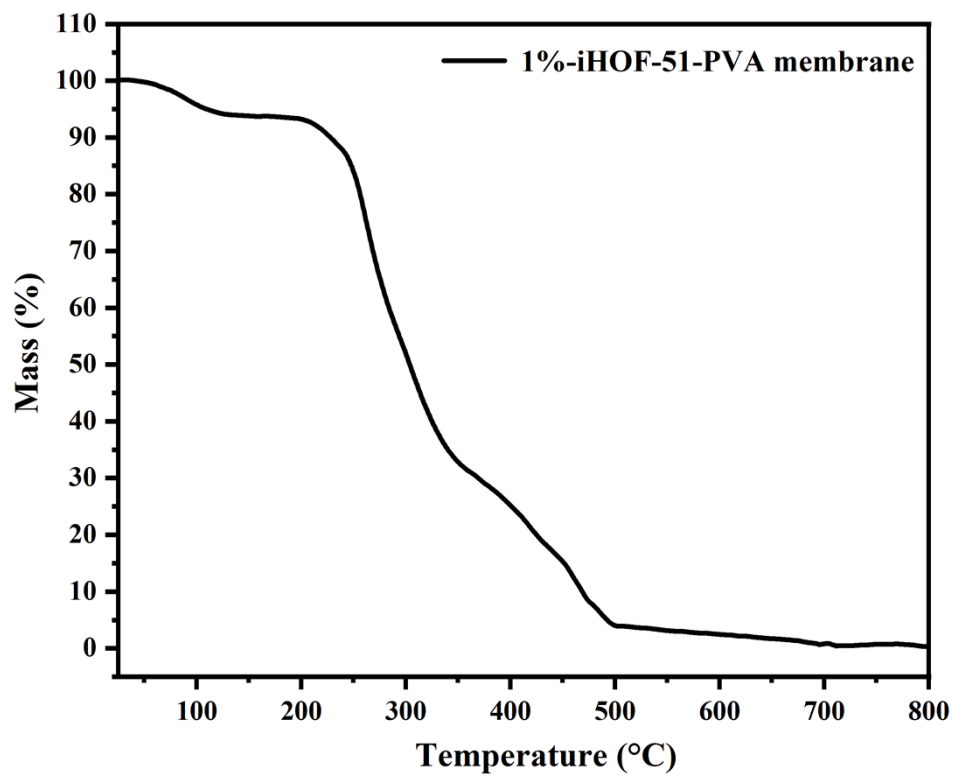


Figure S9. TGA plot of 1%-iHOF-51-PVA membrane.

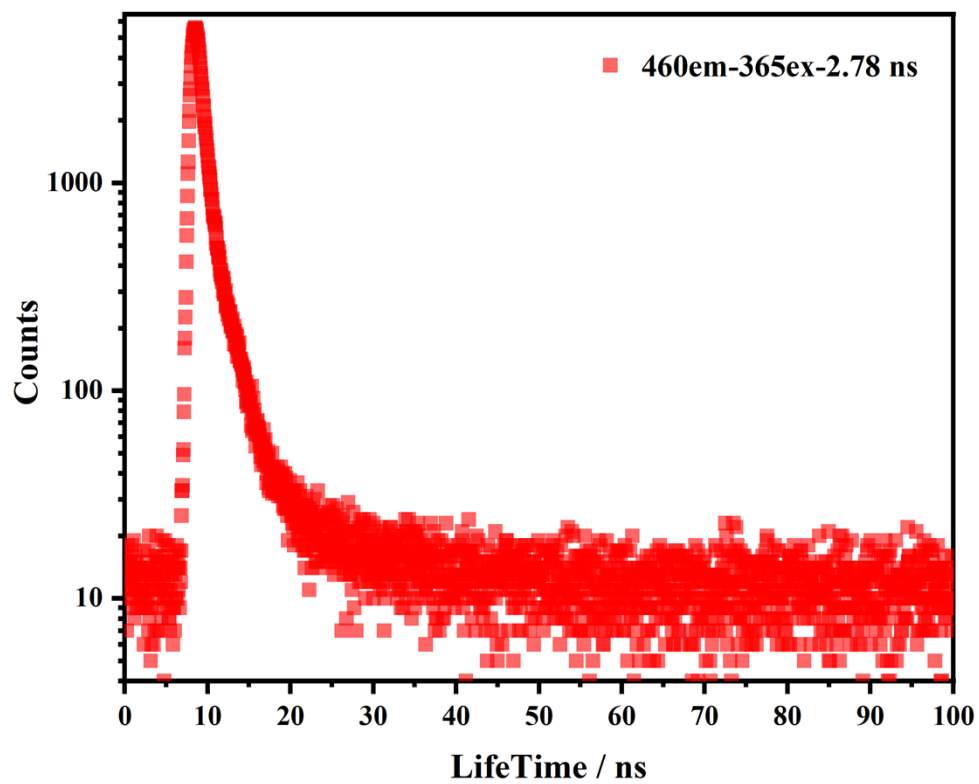


Figure S10. Fluorescence lifetime of iHOF-51 powder.

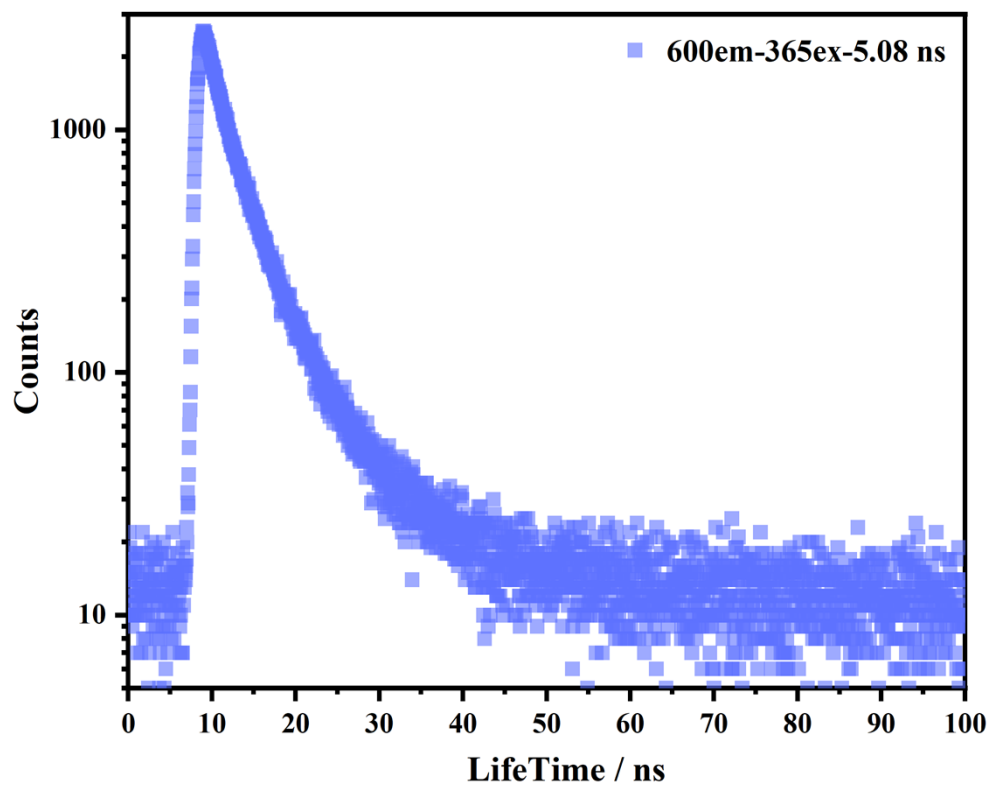


Figure S11. Fluorescence lifetime of 1%-iHOF-51-PVA membrane.

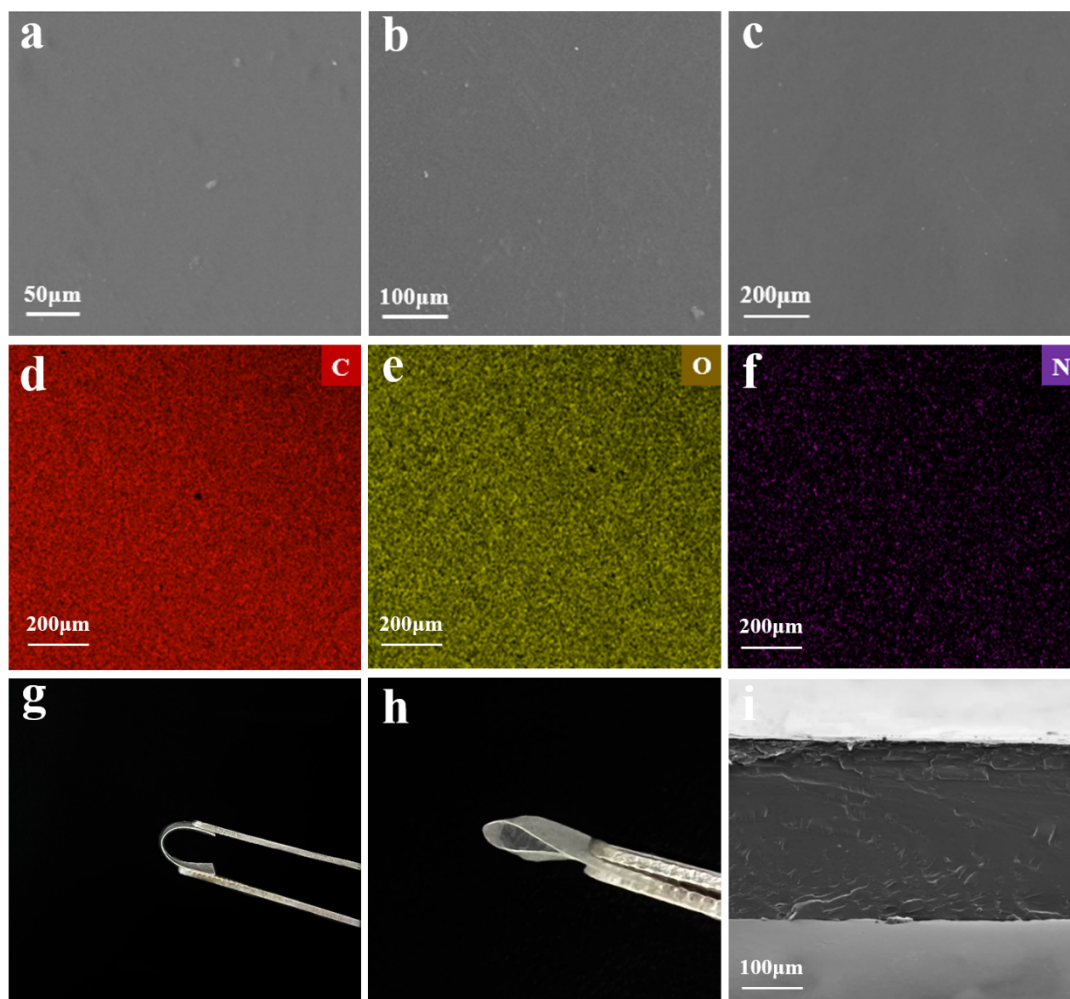


Figure S12. (a-c) SEM images of **1%-iHOF-51-PVA** composite membrane with different magnifications. (d-f) Elemental mapping images of (d) C, (e) O, and (f) N in the **1%-iHOF-51-PVA** composited membrane. (g-h) The bending of **1%-iHOF-51-PVA** composite membrane is different degrees. (i) SEM image of the cross-section of **1%-iHOF-51-PVA** composite membrane.

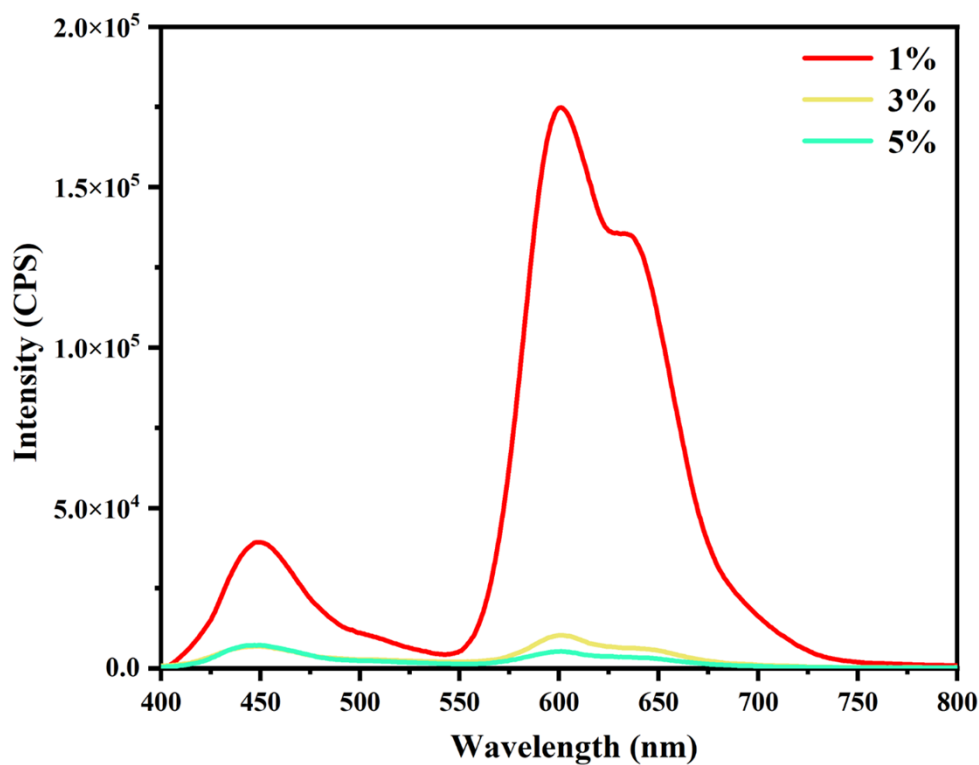


Figure S13. Fluorescence intensity of PVA composite membranes with different doping ratios ($\lambda_{\text{ex}}=365$ nm).

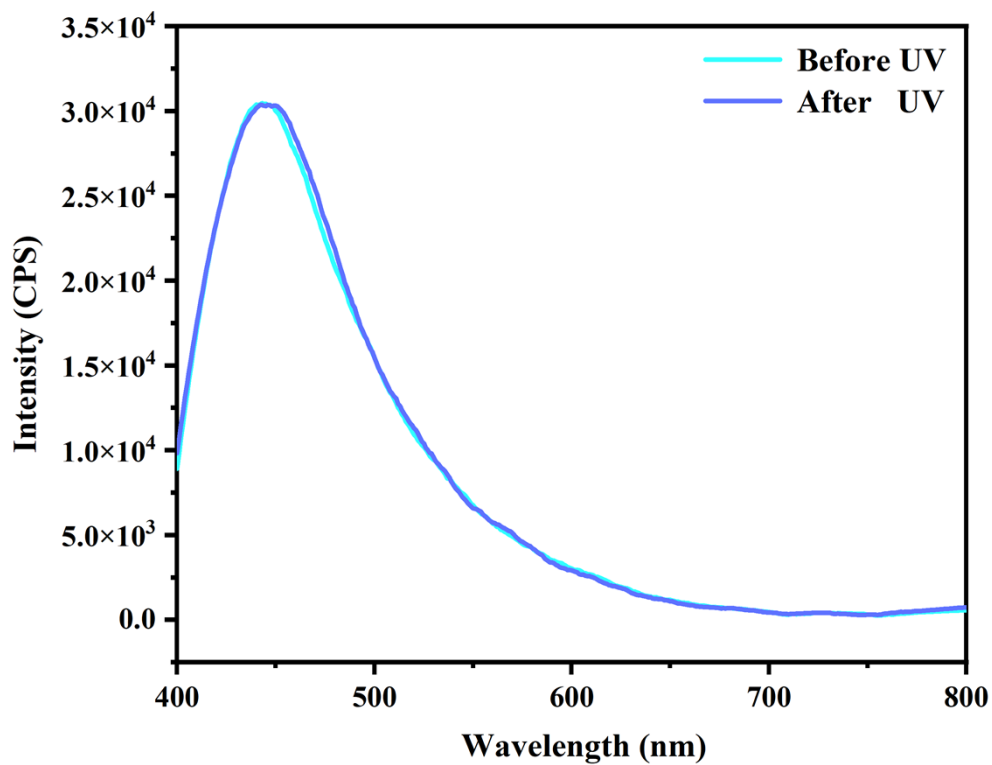


Figure S14. Fluorescence emission spectra of pure PVA membrane ($\lambda_{\text{ex}}=365$ nm).

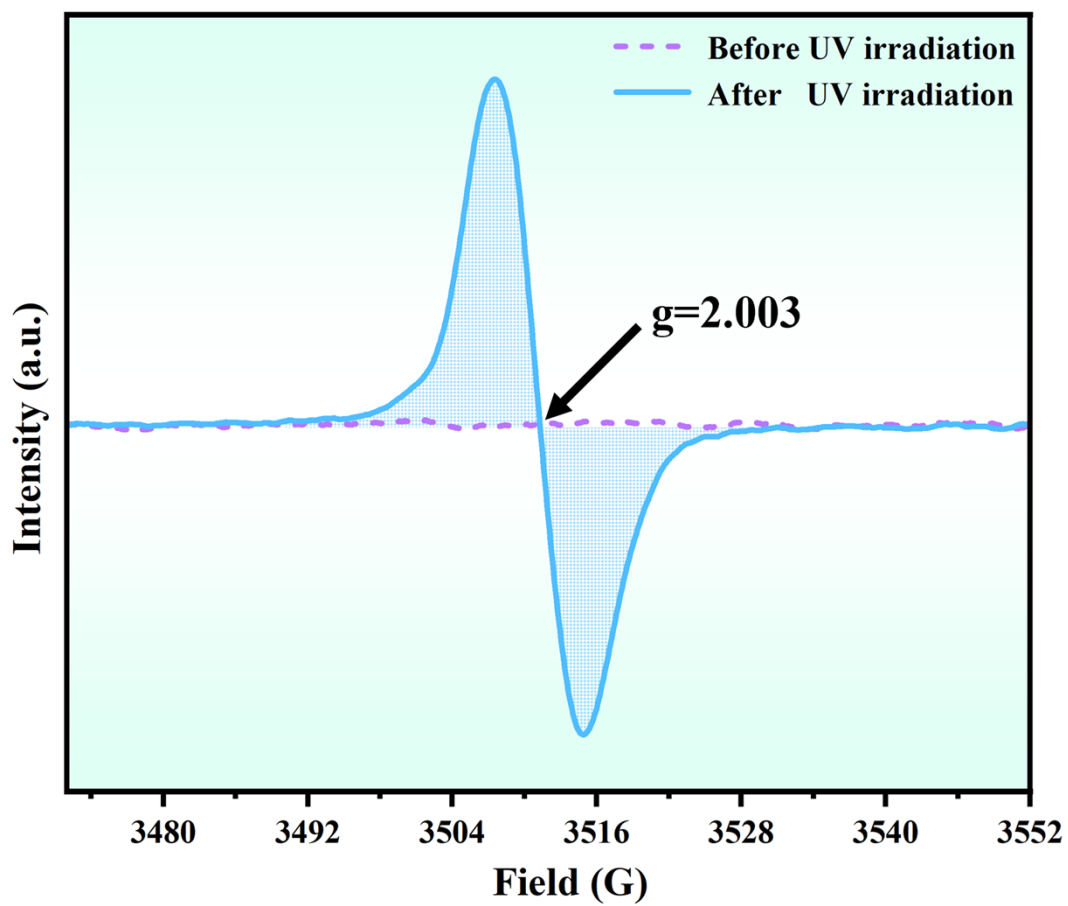


Figure S15. EPR spectra of 1%-iHOF-51-PVA composite membrane before and after irradiation at 365 nm.

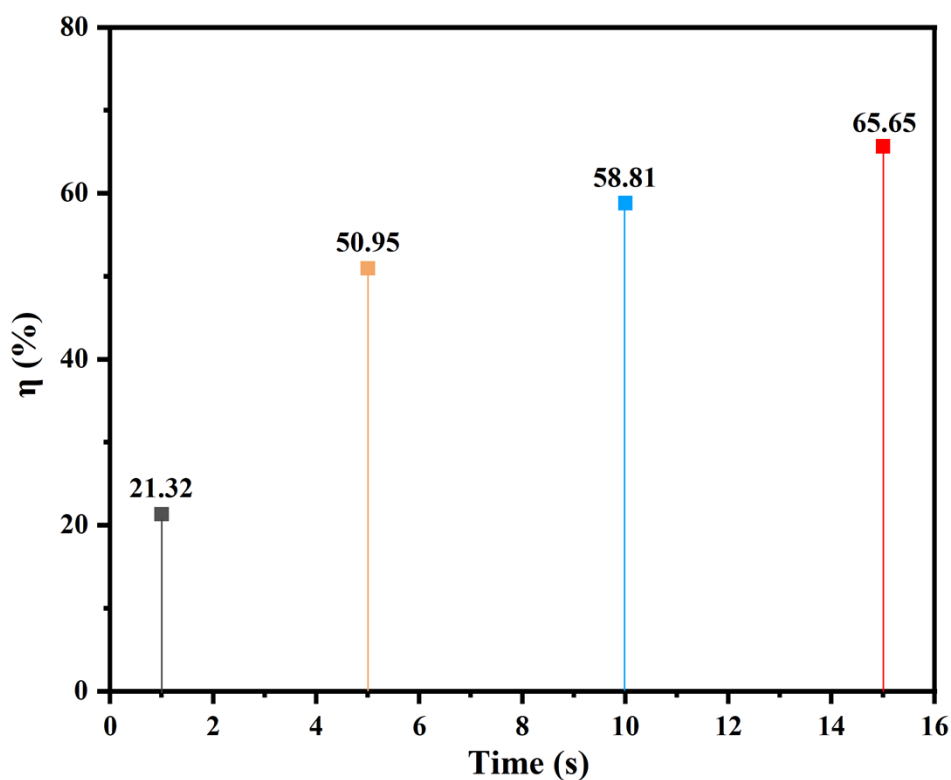


Figure S16. Energy transfer efficiency between PVA and iHOF-51 in composite membrane as a function of irradiation time.

Transfer efficiency

$$\eta = \frac{A_0 - A_t}{A_0} \times 100\%$$

η : energy conversion efficiency; A_0 : initial intensity of fluorescence emission peaks in the complex; A_t : intensity of pure PVA fluorescence emission peaks in the complex corresponding to different times of UV irradiation.

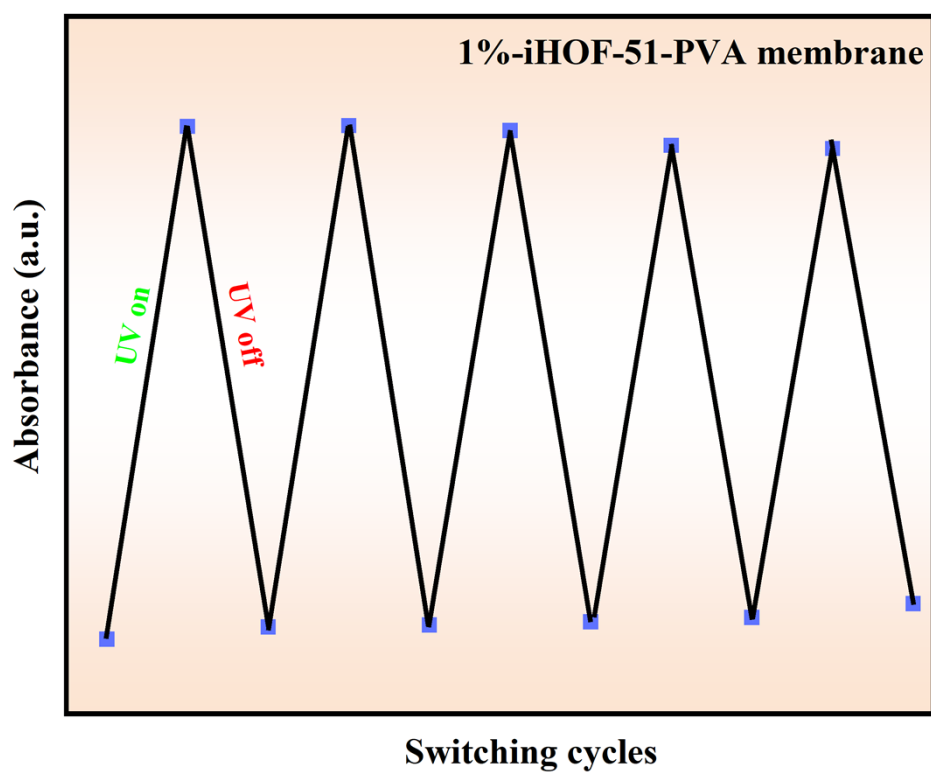


Figure S17. Fatigue resistance of **1%-iHOF-51-PVA** membrane at 365 nm and after re-drying in a high humidity environment.

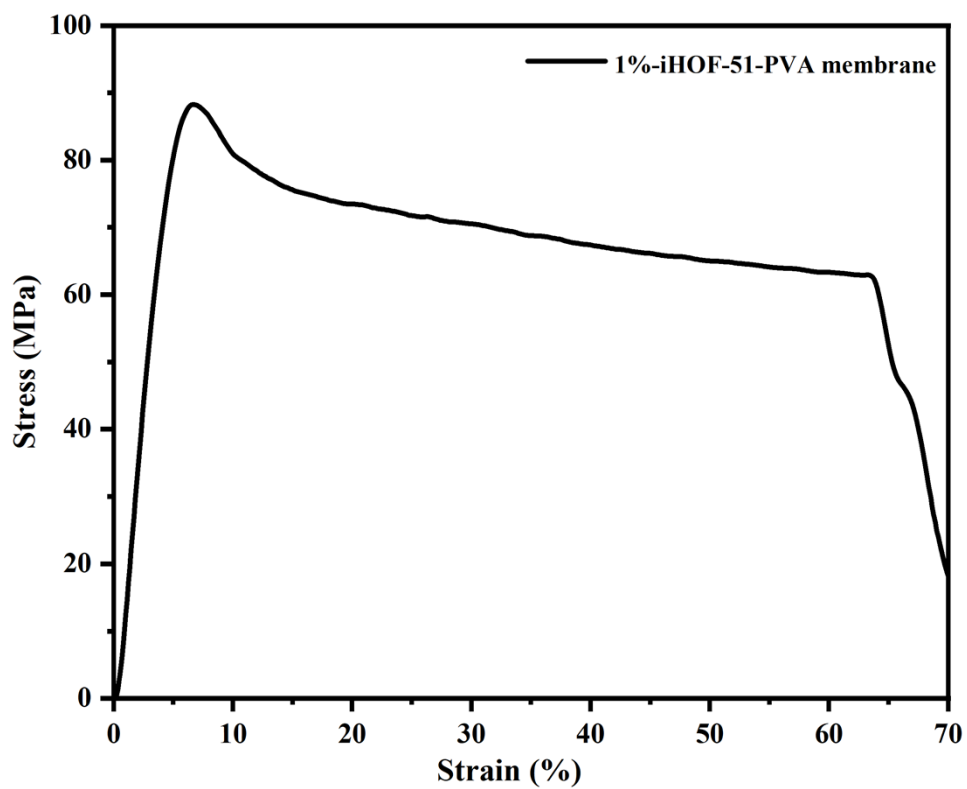


Figure S18. Stress-strain curve of the **1%-iHOF-51-PVA** membrane.

Supporting Tables

Table S1. Crystal structure data and refinement details of **iHOF-51**.

Compounds	iHOF-51
Empirical formula	C ₄₀ H _{36.5} N ₆ O _{10.25}
Formula weight	765.25
Temperature / K	193(2)
Crystal system	trigonal
Space group	<i>R</i> -3
<i>a</i> /Å	30.6005(13)
<i>b</i> /Å	30.6005(13)
<i>c</i> /Å	19.9577(14)
α /°	90.00
β /°	90.00
γ /°	120.00
Volume/Å ³	19.9577(14)
Z	18
ρ_{calc} / cm ³	1.413
μ / mm ⁻¹	0.104
F(000)	7209.0
Reflections collected	109244
Independent reflections	9356
Data/restraints/parameters	9356/997/800
Goodness-of-fit on F ²	1.032
^a R ₁ , ^b wR ₂ [I > 2 σ (I)]	0.1248/0.2913
^a R ₁ , ^b wR ₂ (all data)	0.1827/0.3215
Largest diff. peak/hole / e.Å ⁻³	0.51/-0.37

$${}^a R_1 = \frac{\sum ||F_o| - |F_c||}{\sum |F_o|}, {}^b wR_2 = \left\{ \frac{\sum [w(F_o^2 - F_c^2)^2]}{\sum [w(F_o^2)^2]} \right\}^{1/2}$$

Table S2. List of representative HOF-based photochromic crystal materials.

Crystalline materials	Photoresponsive time	mechanism of photochromism	References
iHOF-51	1 s	free radical	This work
[H₂(bpyb)](H₂PO₄)₂·2H₂O	1 s	free radical	5
PFC-26	2 s	free radical	6
(H₂CV)(H₂BTEC)	3 s	free radical	7
2-NDI	10s	free radical	8
Tb-HOF-2@SP	30s	isomerization	9
[(H₂L) (2,7-NDS)·5H₂O]	30 s	free radical	10
SP2 ⊂ HOF2	60 s	isomerization	11
ECUT-HOF-30	180 s	free radical	12
HOF A	300 s	free radical	13

Table S3. A representative list of PVA-doped photochromic materials.

Crystalline materials/ composite membrane	Photoresponsive time	mechanism of photochromism	References
1%-iHOF-51-PVA	1 s	free radical	This work
10%-iHOF-18-PVA	1 s	free radical	2
TiO₂-006Au/PVA/MB + RhB	3 s	electronic transfer	14
8%-LCPC-PVA	5 s	free radical	15
PVA/d-GCN	60 s	electronic transfer	16
TiO₂/PVA/MB + RhB	120 s	electronic transfer	14
PCNF-PVA-1.0	300 s	free radical	17
10%-iHOF-41-PVA	360 s	free radical	18
5%-iHOF-41-PVA	600 s	free radical	18

Supplementary Reference

- (1) S. Mollick, S. Mukherjee, D. Kim, Z. Qiao, A. Desai, R. Saha, Y. More, J. Jiang, M. Lah and S. Ghosh, *Angew. Chem. Int. Ed.*, 2019, **58**, 1041-1045.
- (2) M-F. Huang, L-H. Cao and B. Zhou, *Chem. Commun.*, 2024, **60**, 3437-3440.
- (3) G. Sheldrick, *Acta Cryst. A.*, 2008, **64**, 112-122.
- (4) G. Sheldrick, *Acta Cryst. C.*, 2015, **71**, 3-8.
- (5) T. Chen, H-B. Jiang, K-B. Jiang, D-L. Hu, L-Z. Cai, M-S. Wang and G-C. Guo, *ACS Appl. Mater. Interfaces.*, 2022, **14**, 11619-11625.
- (6) M. Khanpour, W-Z. Deng, Z-B. Fang, Y-L. Li, Q. Yin, A-A. Zhang, F. Rouhani, A. Morsali and T-F. Liu, *Chem.-Eur. J.*, 2021, **27**, 10957-10965.
- (7) S-L. Li, Y. Shen, W. Yang, Y-J. Wang, Z-K. Qi, J. Zhang and X-M. Zhang, *Chinese J. Chem.*, 2022, **40**, 351-356.
- (8) Y-S. Shi, D-D. Yang, T. Xiao, Z-G. Xia, Y-H. Fang and X-J. Zheng, *Chem. Eng. J.*, 2023, **472**, 145152.
- (9) Y. Gao, Y. Yang, Y. Wei, Y. Li, H. Cai and C. Wu, *Adv. Funct. Mater.*, 2024, 2416025.
- (10) S. Chen, Y. Ju, H. Zhang, Y. Zou, S. Lin, Y. Li, S. Wang, E. Ma, W.

- Deng, S. Xiang, B. Chen and Z. Zhang, *Angew.Chem., Int. Ed.*, 2023, **62**, e202308418.
- (11) Z. He, Y. Li, H. Wu, Y. Yang, Y. Chen, J. Zhu, Q. Li and G. Jiang, *ACS Appl. Mater. Interfaces*, 2022, **14**, 48133-48142.
- (12) L. Wang, L. Yang, L. Gong, R. Krishna, Z. Gao, Y. Tao, W. Yin, Z. Xu and F. Luo, *Chem. Eng. J.*, 2020, **383**, 123117.
- (13) A. Almuhan, G. Orton, C. Rosenberg and N. Champness, *Chem. Commun.*, 2024, **60**, 452-455.
- (14) F. Wang, Y. Song, R. Xie, J. Li, X. Zhang, H. Xie and H. Zou, *Chem. Eng. J.*, 2023, **475**, 146306.
- (15) S. Lin, Y. Tang, W. Kang, H. Bisoyi, J. Guo and Q. Li, *Nat. Commun.*, 2023, **14**, 3005.
- (16) A. Smith, K. Shen, Z. Hou, S. Zeng, J. Jin, C. Ning, Y. Zhao and L. Sun, *Adv. Funct. Mater.*, 2022, **32**, 2110285.
- (17) X. Feng, Y. Tian, G. Gu, C. Wang, S. Shang, X. Huang, J. Jiang, Z. Song and H. Zhang, *Chem. Eng. J.*, 2024, **500**, 156763.
- (18) B. Zhou, L-H. Cao, B-S. Li, X-Y. Chen and X-T. Bai, *ACS Appl. Mater.*, 2024, **16**, 58931-58939.